PNNL-28232

Pacific Northwest
NATIONAL LABORATORY
Proudly Operated by Battelle Since 1965

Material Properties of Zirconium Hydride Phases in Zircaloy-4 Getter Tubes Mapped by Atomic Force Microscopy

October 2018

S Riechers
J Lang
A Guzman
B Johnson
B McCarthy

U.S. DEPARTMENT OF ENERGY

Prepared for the U.S. Department of Energy
under Contract DE-AC05-76RL01830

DISCLAIMER

PACIFIC NORTHWEST NATIONAL LABORATORY
operated by
BATTELLE
for the
UNITED STATES DEPARTMENT OF ENERGY
under Contract DE-AC05-76RL01830

Printed in the United States of America

Available to DOE and DOE contractors from the Office of Scientific and Technical Information,
P.O. Box 62, Oak Ridge, TN 37831-0062
www.osti.gov
ph: (865) 576-8401
fax: (865) 576-5728
email: reports@osti.gov

Available to the public from the National Technical Information Service
5301 Shawnee Rd., Alexandria, VA 22312
ph: (800) 553-NTIS (6847)
or (703) 605-6000
email: info@ntis.gov
Online ordering: http://www.ntis.gov

PNNL-28232

Material Properties of Zirconium Hydride Phases in Zircaloy-4 Getter Tubes Mapped by Atomic Force Microscopy

S Riechers
J Lang
A Guzman
B Johnson
B McCarthy

October 2018

Prepared for
the U.S. Department of Energy
under Contract _____

Pacific Northwest National Laboratory
Richland, Washington 99352

Purpose and Scope

Nickel plated Zircaloy-4 tubing ("getter tubing") is an important functional component in Tritium Producing Burnable Absorber Rods (TBPARs). Getter tubes are used to capture tritium produced during reactor operations and convert it from a gas to a solid by reacting it with Zr to form ZrHx compounds. Previous studies (PNNL-27232, TTP-8-004, and TTP-30710)-on forming Zircaloy-4 hydrides demonstrated that hydride concentration gradients formed under prototypic hydriding conditions and that the microstructure of hydrides formed at 350°C is different than those formed at 500°C, a temperature typically used by the Tritium Technology Program (TTP) for getter rate loading experiments. Differences in hydride distribution, microstructure, and phases were characterize using scanning electron microscopy methods. However, the impact of these differences on material properties is not well understood. The goal of this project was to determine whether atomic force microscopy could observe subtle differences in material properties of single domains of hydride phases formed in Zircaloy-4. These properties include surface structure, hardness, thermal conductivity, and magnetic susceptibility.

Acronyms and Abbreviations

AFM	Atomic force microscopy
FFM	Fast force microscopy
MFM	Magnetic force microscopy
SThM	Scanning thermal microscopy
BSE	Back-scattered electrons
EBSD	Electron back-scattered diffraction
FLG	Full length getter
ID	Inside diameter
OD	Outside diameter
SEM	Scanning electron microscope
SPP	Second phase particles
TPBAR	Tritium producing burnable absorber rod
PWR	Pressurized water reactor
Zr-4	Zircaloy-4 alloy
RMS	Root mean square

Contents

Figures

Tables

1.0 Introduction

Tritium is a valuable hydrogen isotope necessary for various fusion and national security applications. Tritium-producing burnable absorber rods (TPBARs) are used by the U.S. Department of Energy's Tritium Readiness Program to produce tritium when irradiated with neutrons in a nuclear reactor. The exterior of the TPBAR is a stainless-steel tube and the internal components have been designed and selected to produce and retain tritium. Within the stainless-steel cladding is a tube made of nickel-plated Zircaloy-4 that encircles a stack of annular, ceramic pellets made from lithium aluminate. This tube is used to getter the tritium gas produced in a TPBAR by forming solid-phase hydrides within the tube. A schematic of a TPBAR and a photograph of a $LiAlO_2$ pellet is shown in Figure 1. The pellets are enriched with the ^6Li isotope. When irradiated in a PWR, the ^6Li in the pellets absorbs neutrons, undergoes a neutron capture reaction, and produces tritium and helium as a result. The tritium chemically reacts with the Zr metal getter, which captures the tritium as a metal hydride. This capture process minimizes the pressure build-up in the TPBAR, and also limits the diffusion of tritium out of the TPBAR into the reactor coolant. Efficient adsorption of tritium is an important performance criterion for getter tubes, thus the hydriding process is an important area of study for the Tritium Technology Program.

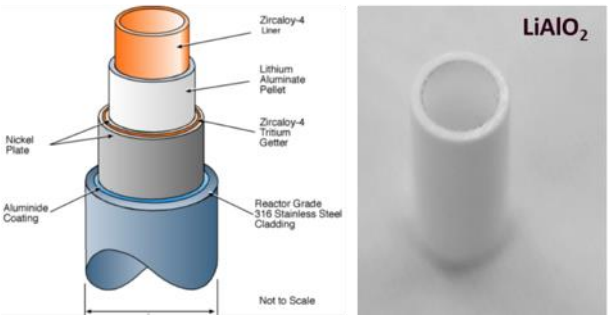

Figure 1. Schematic of TPBAR and photograph of $LiAlO_2$ pellet.

The distribution of hydrides in irradiated getter tubes is not well understood. Variations in color have been observed in post-irradiated getter tubes. The variations in color are assumed to be due to variations in hydride or carbon content. At one time, it was assumed that prolonged time at reactor temperatures, and exposure to steady neutron fluxes would provide sufficient opportunity for hydrides to form homogeneously and/or diffuse throughout the getter tubes. However, previous experimental evidence indicated that this assumption was not valid.[1,2,3] These experiments explored the effect of hydriding conditions (immersion versus internal), temperature, D_2 versus H_2, and bare versus nickel plating have on the resulting distribution, microstructure and phase of hydrides. Over the course of these experiments it was discovered that hydride concentration gradients do form under prototypic hydriding conditions and that the microstructure of hydrides formed at 350°C is different than those formed at 500°C, a temperature typically used for simulant hydriding. The differences in hydride distribution, microstructure, and phases were characterize using scanning electron microscopy methods. However, the impact of these differences on material properties is not well understood. In this report subtle differences in material properties of hydride phases formed in Zircaloy-4 are mapped onto local topography using atomic force microscopy. The relative hardness, thermal conductivity, and magnetic susceptibility are measured in relation with the surface structure of individual hydride domains.

2.0 Experimental Set up

Hydrided zirconium tubing was prepared by exposing both bare and nickel-plated Zircaloy 4 to hydrogen or deuterium gas. Two different approaches for hydriding Zr-4 tubing were evaluated. The original method used by the Tritium Technology Program for hydriding Zr tubes is called "immersion hydriding". It was developed to evaluate the rate of hydrogen gettering in zirconium alloy tubes. This original hydriding apparatus is sometimes called the "getter rate" furnace. For the purpose of more closely simulating reactor conditions, and in an attempt to create hydride concentration gradients, a new hydriding apparatus was developed. This test method was called "prototypic hydriding", and was designed to simulate many of the conditions that a getter tube would experience during reactor operations.

2.1 Immersion Hydriding

A picture of the immersion hydriding test apparatus is shown in Figure 2. This equipment set up is sometimes called the "getter rate" furnace. This was the apparatus used for the previous hydriding studies[1,2,3]. This process is typically used to test the rate at which getter tubes react with hydrogen gas to form hydrides.

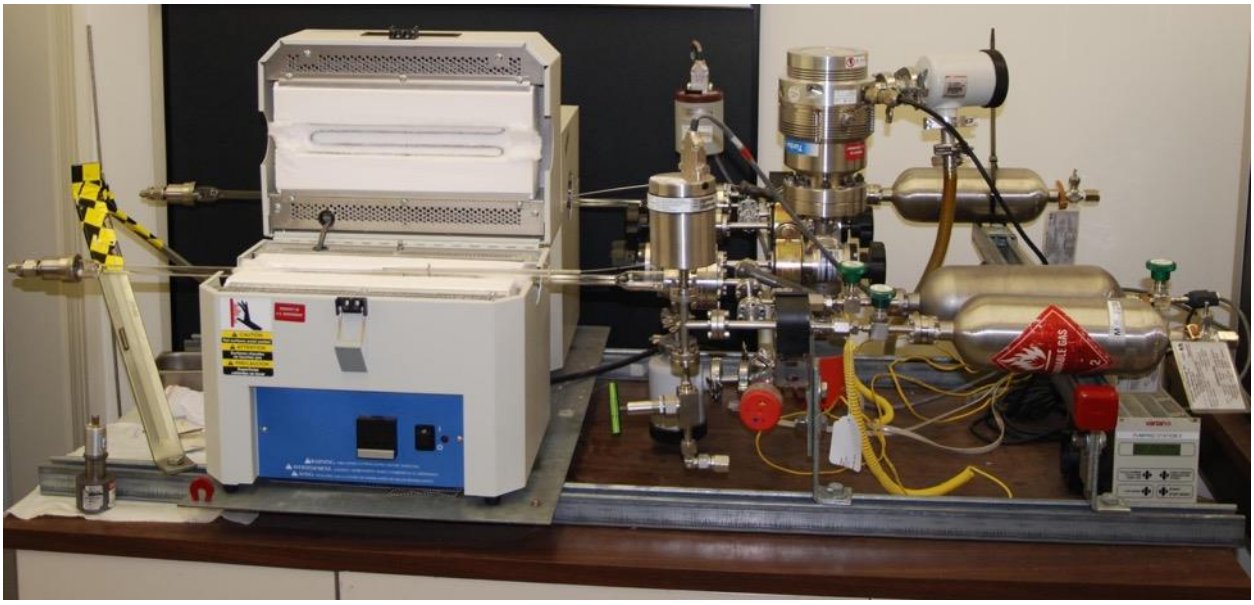

Figure 2. Immersion hydriding test apparatus used for getter rate testing.

Getter tubing was hydrided by placing two inch tubing sections into a quartz tube furnace. The quartz tube was evacuated to less than $1x10^{-4}$ Torr and then heated to 500°C in a vacuum. Hydrogen was leaked into the system at a fixed leak rate $4.5x10^{-8}$ mol/second. The level of hydriding was controlled by regulating the amount of time that the getter tube was exposed to deuterium gas. The pressure in the system was continuously monitored and used as an indication of hydrogen uptake by the Zr tubing.

2.2 Prototypic Hydriding

2.3

A new experimental test set up was designed to hydride getter tubing under prototypic reactor conditions. The key features were to introduce deuterium gas only to the interior of the getter tube, while maintaining the outside of the tube under vacuum and at prototypic reactor temperatures (e.g. ~ 350°C). Additionally, it was desired to create diffusion gradients radially (through the thickness) and longitudinally (along the axis of the specimen). This apparatus was called "prototypic hydriding".

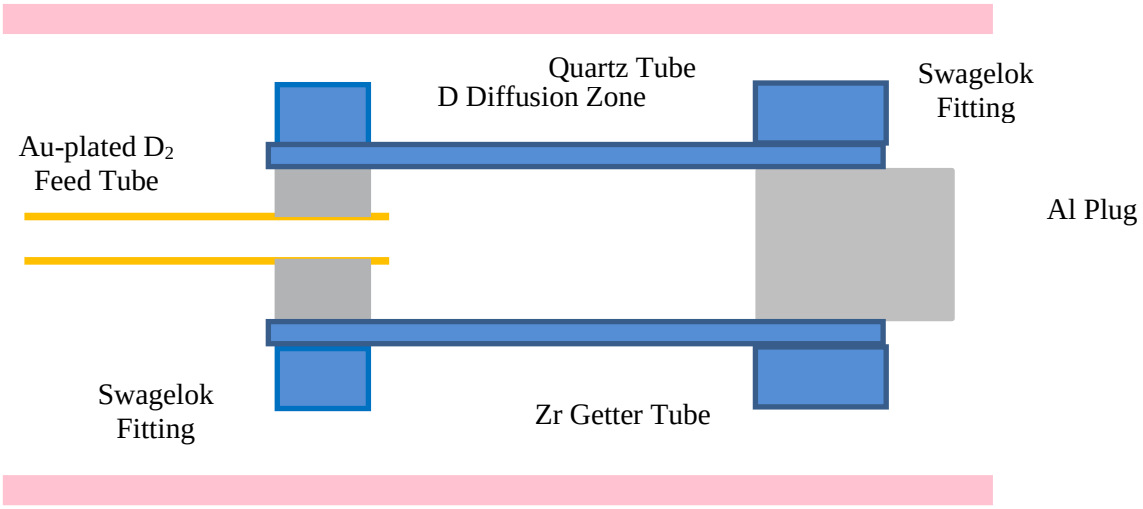

Figure 3. Schematic of the prototypic hydriding test configuration used to study the formation and morphology of zirconium hydrides in nickel plated getter tubes.

A schematic of the prototypic hydriding test apparatus is shown in Figure 3. A 2" long specimen was cut from a finished full-length getter (FLG) tube. It was sealed on one end through a Swagelok reducer fitting to the "feed tube" - a 1/8-inch OD gold-plated, stainless steel tube. The other end of the sample was plugged with a close-fitting aluminum plug extending about ½ inch into the sample, and constrained by additional swage lock fittings. Deuterium was used as a surrogate for tritium. Introducing deuterium only into the interior of the Zr-4 tube simulates the production of tritium by the $LiAlO_2$ pellet in a TPBAR. The specimen was heated to 350°C to more closely simulate actual reactor operating temperatures.

Figure 4. Specimen with Swagelok fittings on both ends attached to Au-plated stainless steel tubing for hydrogen supply.

Once assembled, the apparatus was placed inside a quartz tube and into a tube furnace (Figure 5 and Figure 6). The quartz tube was connected to a vacuum pump and a gas manifold to permit evacuation of the exterior of the test assembly and purging with argon gas. The 1/8-inch tubing was connected to a deuterium gas bottle fitted with a controlled leak rate orifice to provide a low and constant flow of deuterium gas (2.7×10^{-8} mol/s) to the interior of the sample.

Figure 5. Assembled Test Article inside the quartz tube in the tube furnace.

Figure 6. Over-view of the prototypic hydride loading apparatus.

The interior of the sample was initially evacuated to about 1×10^{-6} torr, and the sample was heated to 350°C for about ten minutes to allow ample time for the aluminum plug to swell and seal the getter tube. Then the deuterium bottle was opened allowing deuterium to pressurize the inside of the sample. Specific

level of hydriding were achieved by controlling the amount of time that the specimen was held at temperature while being exposed to the deuterium gas. For example, a specimen maintained at these conditions for about 4 days – would have an estimated D/Zr mole ratio ~ 1.0. The furnace was then cooled down and the assembled test article was removed. The sample was disassembled and prepared for microstructural examination.

3.0 Sample Preparation

Two different approaches were used to prepare specimens for AFM/SEM analysis. The first approach relied on traditional mechanical polishing methods. The second approach was a newer technique that used a high energy, focused beam of Ar ions to mill the specimen and create a cross-section specimen.

3.1 Mechanical Polishing

The typical approach used to prepare specimens for AFM/SEM examination is to mechanically polish them using a series of successively finer abrasives and polishing pads. Since there is interest in understanding the microstructure of irradiated getter tubes, the same type of sample preparation equipment that would be used for irradiated specimens was used for this project. An example polishing protocol using a small, single-specimen random orbital polishing machine (Buehler MiniMet) is shown in Table 1.

Table 1. Example polishing protocol used for epoxy-mounted, hydrided Zircaloy-4 tubing using a single-sample, random orbital polisher.

Time	Speed	Load	Pad	Abrasive
5 min	30	5 lb	SiC	120 grit; Oil lubricant
8 min	30	3 lb	SiC	240 grit; Oil lubricant
8 min	30	3 lb	SiC	400 grit; Oil lubricant
8 min	30	3 lb	SiC	600 grit; Oil lubricant
30 min	30	3 lb	Plan*	9um diamond suspension in propylene glycol*
30 min	30	3 lb	White Label*	3um diamond suspension in propylene glycol*
30 min	30	3 lb	White Label*	1um diamond suspension in propylene glycol*
30 min	30	3 lb	White Label*	CMP** (Chemical Mechanical Polishing compound; mixture of colloidal SiO_2 and colloidal Al_2O_3)
30 min	30	3 lb	Final P*	Acidic Colloidal Alumina**
30 min	30	3 lb	White Label*	CMP**
30 min	30	3 lb	Final P*	Master Polish 2$

*Sold by Allied High Tech; **Sold by PACE Technologies; $Sold by Beuhler

3.2 Ion Milling

Cross-section ion milling was a second method used to prepare specimens for analysis. This method uses a high energy argon ion beam to erode away material from the specimen via ion bombardment. A flat piece of very hard metal (the shield plate or masking plate) is placed on top of the specimen so that only a small thin (20 – 80 µm) region is exposed to the ion beam. The Ar ions bombard the specimen from above, eroding away material, thereby creating a polished cross section from the exposed region. During the milling process, the specimen can be rocked to help reduce curtaining (non-uniform surface) artifacts and increase polished area. Figure 7 shows a series of cartoons illustrating the operation of a JEOL cross section polisher, which was used for this project.

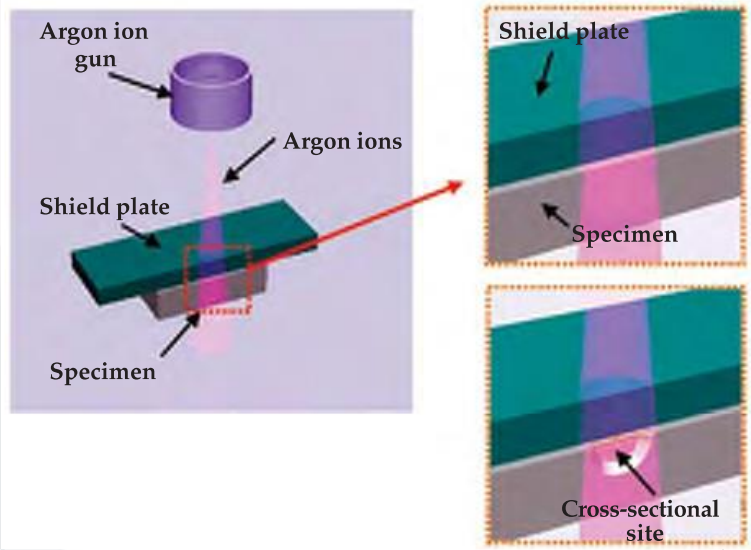

Figure 7. Cartoon showing the operation of a JEOL cross-section polisher tool

The benefit of ion milling is that it is able to produce cross section specimens without the artifact of chemical reactions between the polishing compounds and the specimen. The alpha phase regions in the ion milled specimen have fairly uniform gray scale contrast, and the boundaries between different grains are readily apparent. Another advantage of cross section ion milling is that there is significantly less labor involved with sample preparation. An ion milled specimen can be prepared in about an hour, and then milled overnight. A traditionally polished specimen must first be mounted in epoxy (which is typically cured overnight) and then polished, which is an additional 4-5 hours at a minimum. The disadvantage of ion milling, though, is that the specimen ends up with long vertical variations or undulations in topography. This is called "curtaining" and is due to the streaming flow of ions across the surface of the specimen encountering regions of different hardness. A harder region erodes slower than an adjacent area, thereby leaving a long bump in the wake of the flow of ions. Contamination of the specimen by Ar or the masking plate has not been observed to date.

4.0 Scanning Electron Microscopy

A table showing the two specimens selected for SEM/AFM analysis for this report is shown in Table 2.

Table 2. Table of Zr-4 Specimens Hydrided and Selected For AFM Analysis

Sample Name	Hydriding Method	Ratio	Plating	Temperature	Surface Preparation
Getter Rate	Immersion	H/Zr: 0.67	bare	500°C	Mechanically Polished
Prototypic	Prototypic	D/Zr: 0.50	Nickle Plated	350°C	Ion Milled

4.1 Getter Rate Mechanically Polished ZrH_x

The microstructure shown in Figure 8 is somewhat complicated, however EBSD analysis (Figure 9) of a different specimen with similar hydrogen loading was used to interpret the different features. The un-hydrided Zr with a limited amount of soluble hydrogen in it is called the "alpha-phase". An outline of an alpha phase grain is shown in Figure A and shown in green in Figure 9. In BSE mode, contrast is derived based on average atomic number. Since the hydride regions have a lower average atomic number, they show up much darker than the alpha phase. A polycrystalline region of hydrided material is shown in Figure B. There are several different zirconium hydride phases possible (γ, δ, ε, and ζ), depending on the concentration of hydrogen in the specimen. The variation in gray scale contrast in the hydride region is an indication that there may be more than one hydride phase present.

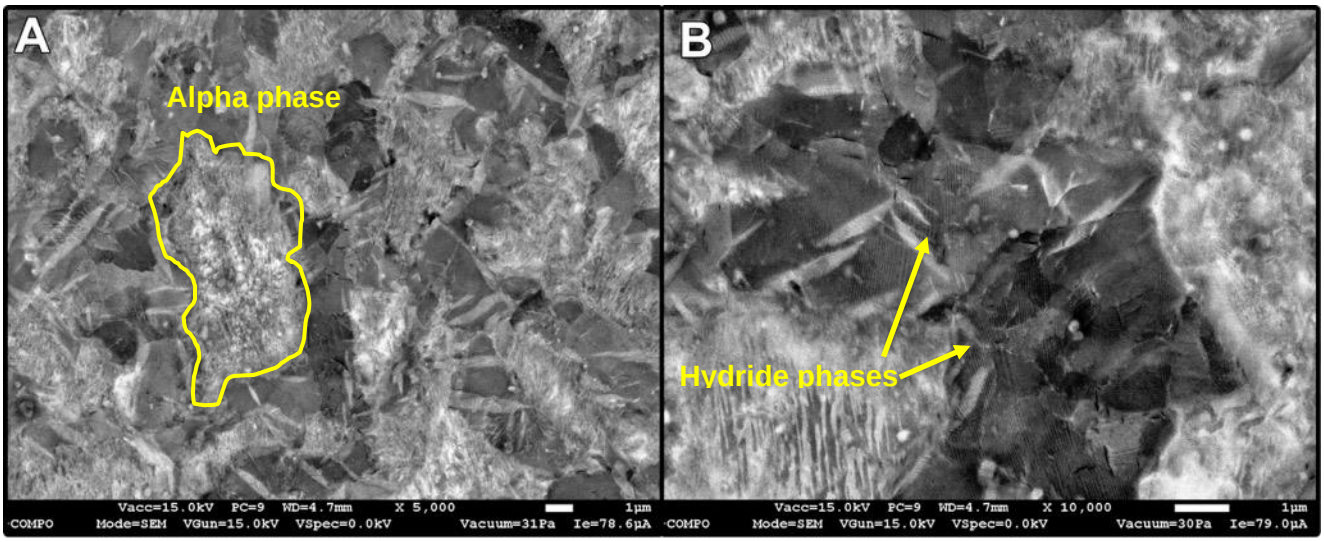

Figure 8. SEM BSE micrographs of a Zircaloy-4 getter tube hydrided to H/Zr ~0.67. Specimen was polished using traditional mechanical polishing methods.

The EBSD phase map in Figure 9 shows the distribution of the three different phases in this specimen.

One of the liabilities of this sample preparation method is that the zirconium tends to react with the polishing chemicals to form hydrides and oxides on the surface. Typically, one would expect a single-phase region like the alpha-phase zirconium grains to have a single solid gray scale appearance. Note however that in Figure 8 the alpha phase grains have a mottled appearance. This is an indication that the surface of the specimen was somehow chemically modified during the polishing process. Multiple

different polishing compounds and methods have been evaluated, both aqueous and non-aqueous, but no liquid-based, mechanical polishing process has been found (during the course of this project) that was free of these chemical modification effects.

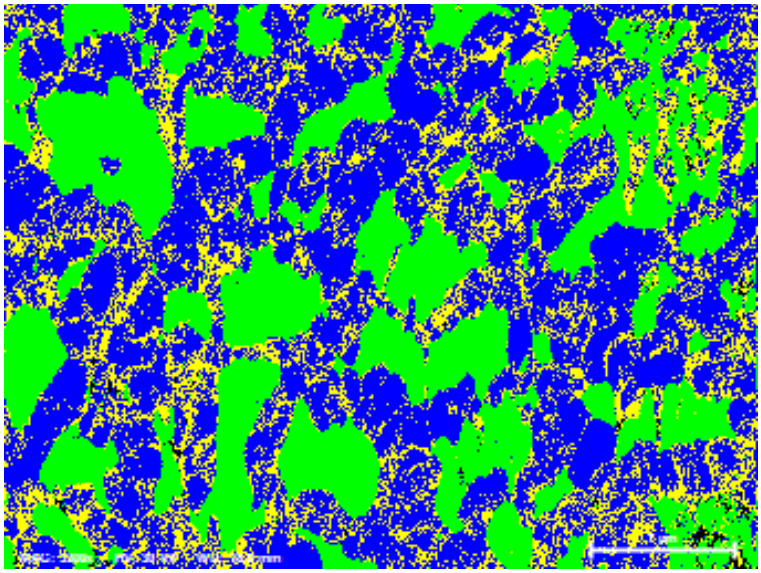

Figure 9. EBSD phase map of a Zircaloy-4 getter tube hydride with H/Zr ~ 0.67. Green = alpha zirconium; blue = delta phase, and yellow = gamma phase.

4.2 Prototypic Ion Milled ZrH_x

A Ni-plated getter tube loaded with deuterium under prototypic conditions at 350°C to a level of D/Zr ~ 0.5. The gas inlet was on the left, and an Al plug was on the right. A specimen for SEM examination was sectioned from the getter tube approximately 25 mm from the Al plugged end of the tube. A montage of SEM BSE micrographs showing the ion milled cross-sectioned area is shown in Figure 10. The specimen was oriented such that the ID of the tube was up, the OD was down, and the gas flow was from left to right in the figure. In general, there was a higher concentration of hydrides along the ID surface than along the OD surface. The hydrides that form at 350°C are needle-like in shape, and tend to form in clusters, with multiple hydrides in a given grain, Figure 11. The hydrides tend to stop or become deflected when they encountered a grain boundary. Their distribution is not uniform; one grain might have several hydrides in it, while adjacent grains, above and/or below it might not have any. Multiple hydrides in a given grain tend to form parallel to each other. In some cases the number of hydrides in a given grain are so high that the hydrides almost completely filled the grain, Figure 11D. Even in those situations, the grains are not fully hydrided and thin bands of un-hydrided residual alpha phase remained.

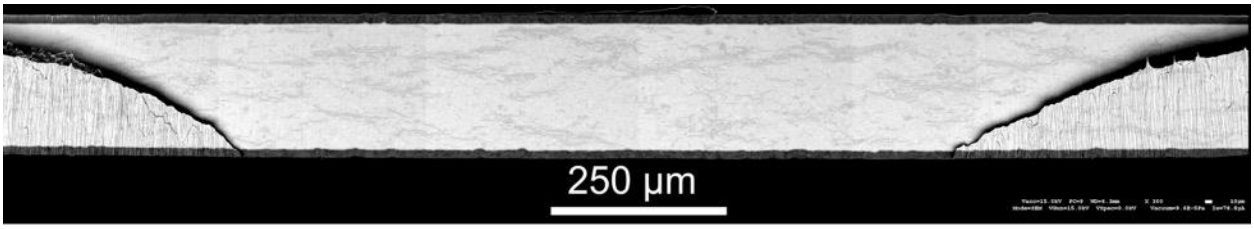

Figure 10. Montage of SEM BSE micrographs of a Ni-plated Zircaloy-4 tube loaded with D_2 under Prototypic conditions to a level of D/Zr ~ 0.5. Specimen was taken towards the plugged end of the tube.

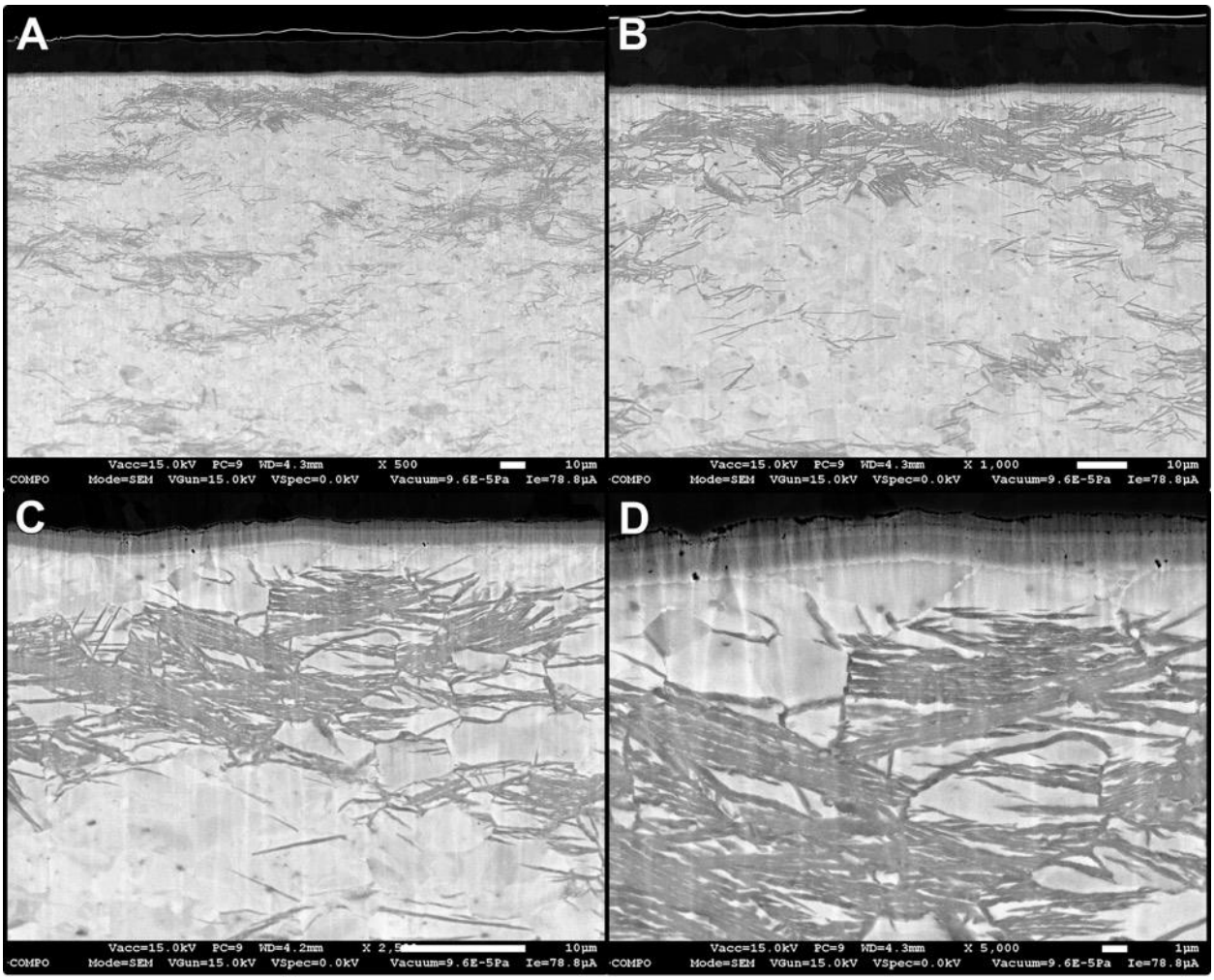

Figure 11. SEM BSE micrographs from near the plugged end of a Ni-plated Zircaloy-4 tube loaded with D_2 under prototypic conditions to a molar ratio of D/Zr ~ 0.5. Micrographs were near the ID of the tube.

4.3 ZrH_x Twinning

The twinning is observed as very small parallel lines of alternating contrast in the hydride grains. Twinning is the term used to describe a situation where two adjacent crystals, with different orientations, share a common set of crystal lattice points. Multiple crystal twins that occur parallel to each other are

called polysynthetic twins, and when these twins are closely spaced to each other, they appear as striations or fine parallel lines.[4] When Zr hydrides, the hydrogen occupies tetrahedral sites in the Zr lattice. The hydrogen addition changes the shape of the crystal lattice. Since the hydride grain is constrained by the adjacent alpha phase Zr grains, it is not able to freely change its shape to accommodate the additional hydrogen. Thus strain builds up in the hydride grain. Polysynthetic twinning is one way that the strained hydride grain can relieve some of the built up strain. Twinning microstructures are commonly observed in hydride grains at high magnifications in specimens where there is a region with a high concentration of hydrides in samples prepared under Getter Rate or Prototypic conditions, Figure 12.

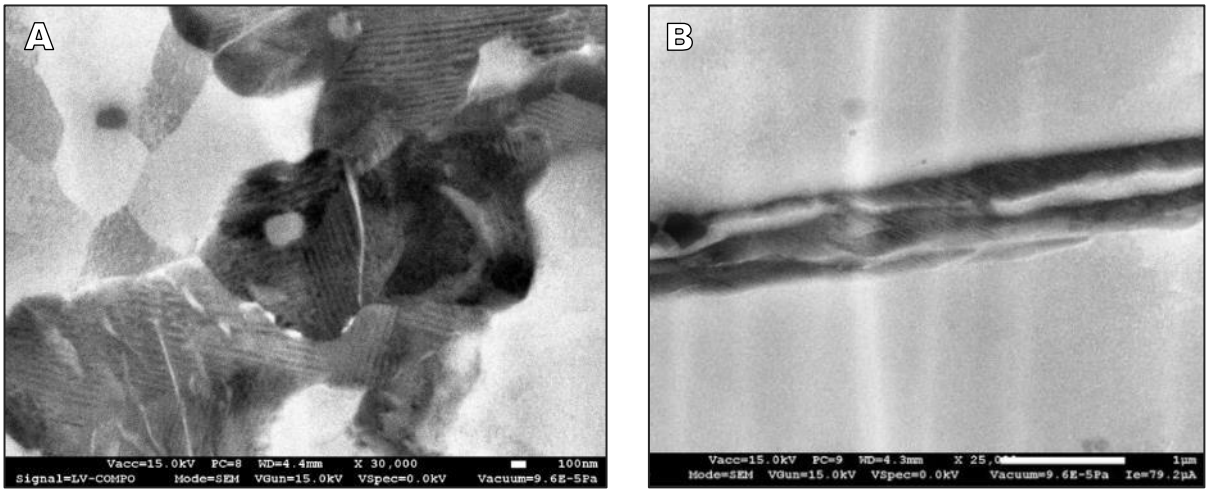

Figure 12. Twining present in hydrides formed under Getter Rate (H/Zr ~ 0.88) (A) and Prototypic (D/Zr ~ 0.5) (B) conditions.

5.0 Atomic Force Microscopy

A new MFP-3D Infinity Asylum Research/Oxford multimodal AFM was used for this study. AFM is a scanning probe microscopy technique in which a sharp tip (2-50 nm in diameter at the apex) attached to a cantilever is rastered laterally across a surface up to 90 µm with sub nanometer precision. A laser is reflected off the back of the cantilever in order to measure the deflection of the cantilever. The deflection of the cantilever is proportional to the force applied by the tip. A set-point deflection is selected and held constant by a feedback loop such that the tip glides across the surface with a constant force. The relative height of the tip during a scan provides the topography of the surface. During a single scan many "channels" are captured simultaneously. For instance the relative vertical movement of the tip provides the "deflection" channel image that highlights surface edges. By utilizing specialized tips and modified scanning procedures many local material properties can be used as the feedback parameter or measured passively as additional channels and overlaid onto the topography. These properties include hardness, adhesion, magnetic domains, thermal conductivity, electrical conductivity, surface charge, piezo response as well as many others.

5.1 Sample Preparation for AFM

The ZrH_x sample preparation methods listed above were developed for SEM and are well suited to that purpose. However, AFM is sensitive to surface contamination, especially organic, that does not affect SEM imaging. Thus, residues left behind after processing or accumulated over time must be removed before AFM imaging. Figure 13A-B show optical images taken from the AFM before and after cleaning a ZrH_x sample by gently swiping first a kimwipe soaked in methanol across the surface followed by one soaked in acetone. The tip cantilever can be seen above the sample with the laser focused on the backside of the region where the tip is located. Figure 13C-D are AFM images that exhibit the streaking effect commonly caused by the presence of sub-monolayer organic contamination.

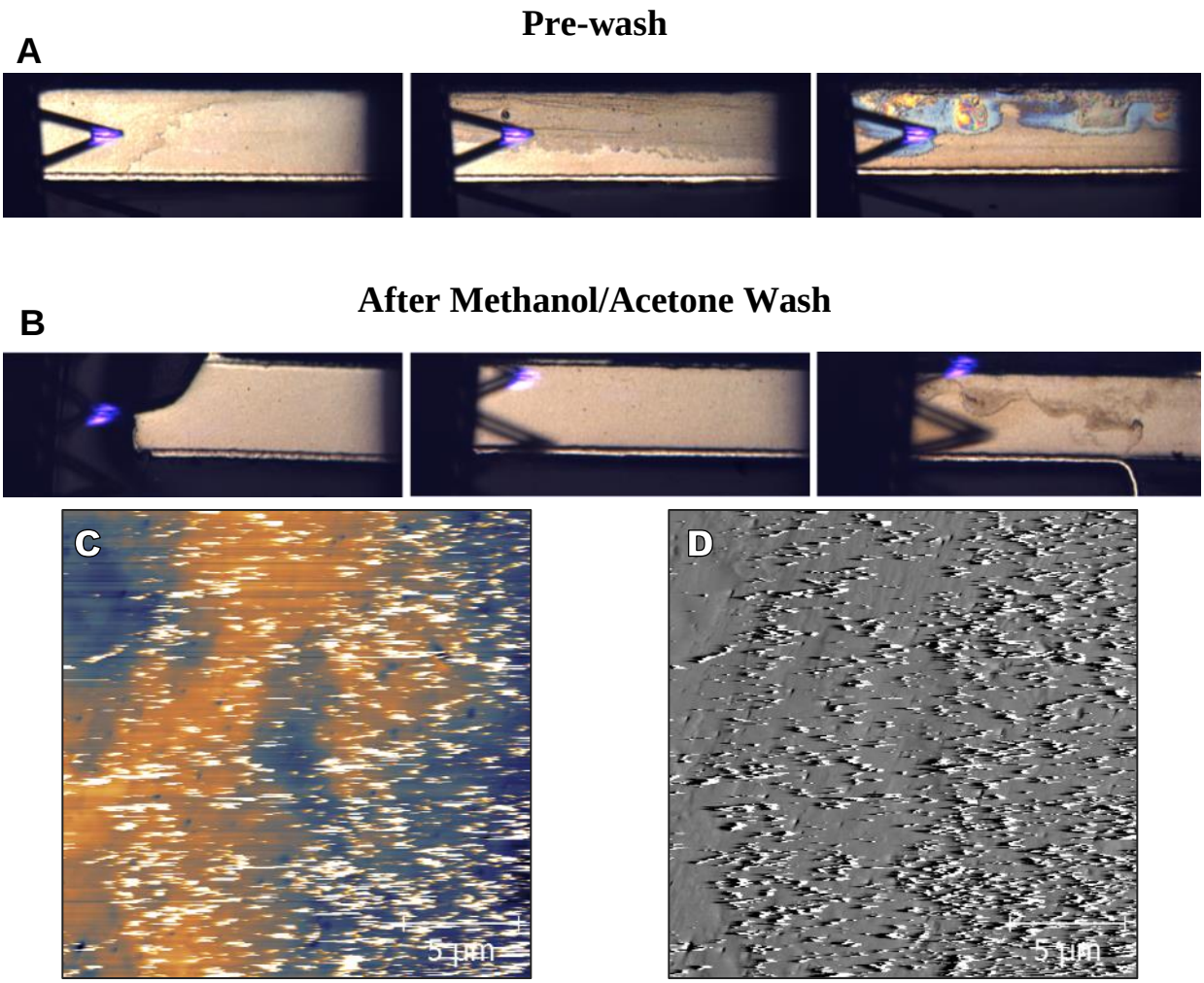

Figure 13. Optical images of a mechanically polished hydrided Zr-4 surface before (A) and after (B) additional cleaning for AFM imaging. The streaking effect caused by surface contamination during AFM imaging can overwhelm the surface features in topography (C) and deflection (D).

5.2 Getter Rate Hydriding, Mechanically Polished

AFM imaging of the Getter Rate sample, a bare Zircaloy-4 getter tube hydrided via immersion in H_2 at 500°C to a 0.69 H/Zr atomic ratio is shown in Figure 13. The sample was polished according to the protocol describe in section 3.1 resulting in a peak to valley height of ~20 nm and RMS of 7.5 nm, Figure 13C. A region with a high degree of twinning is immediately apparent in the deflection images. At higher resolution, Figure 13G, at least 3 different forms of twinning are present in the same region. One of these twinning regions (3) consists of larger ridges ~ 5 nm tall separated by 200-300 nm which are corrugated along only one side with ~ 0.2 nm ridges separated by 20-30 nm, Figure 13H-K. The hierarchical nature of the twinning structures becomes more apparent when viewed as a 3D projection of the topography, Figure 13L.

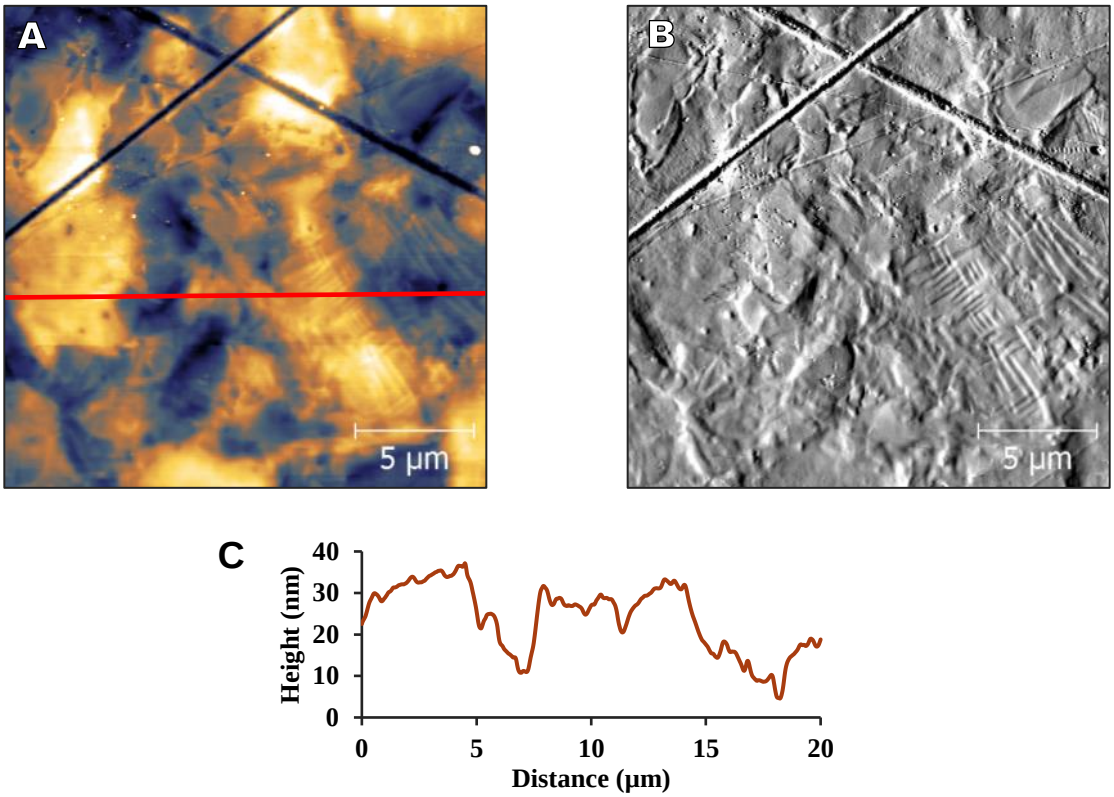

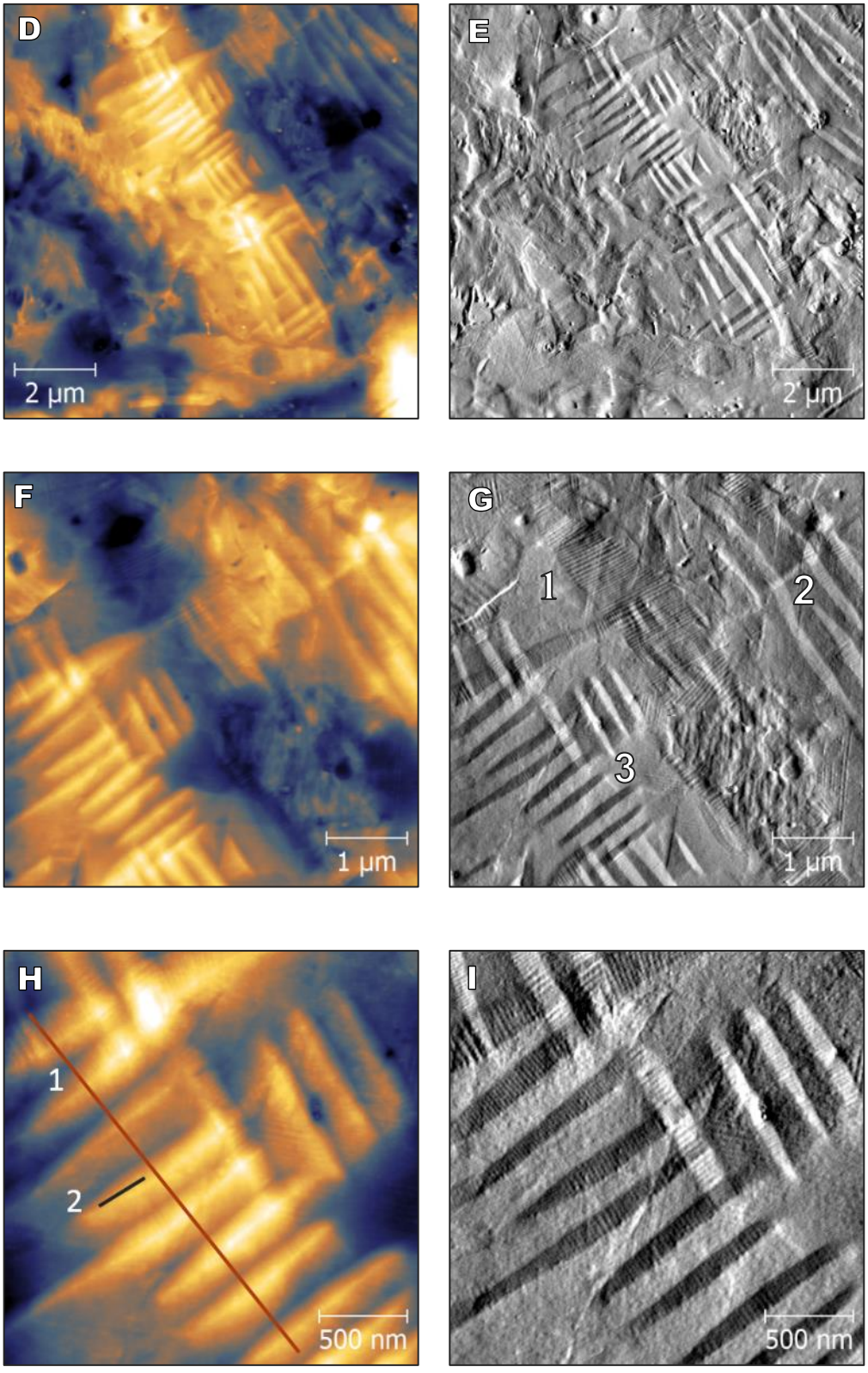
D
2 µm
E
2 µm
F
1 µm
G
1
2
3
1 µm
H
1
2
500 nm
I
500 nm

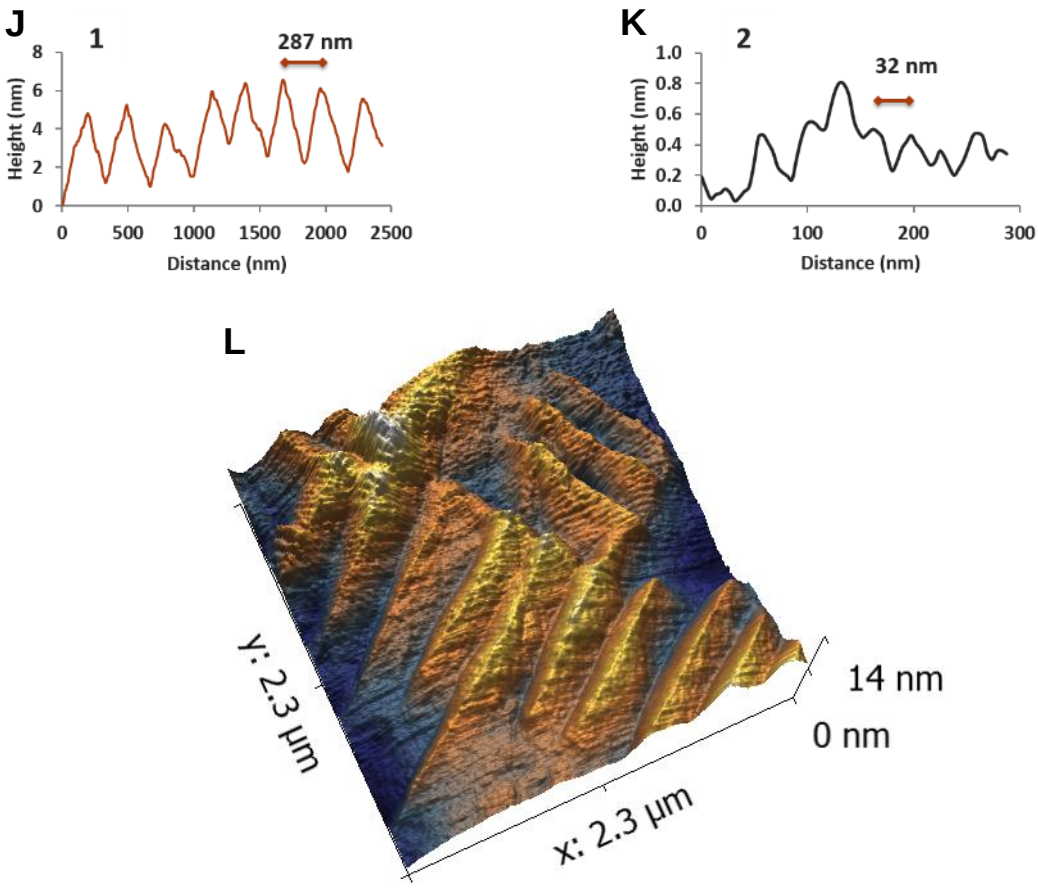

Figure 14. AFM topography (A, D, F, H), deflection (B, E, G, I), and 3D projection (L) images of twinning features present in a mechanically polished Zr-4 sample hydrided at 500°C. The overall surface roughness large twinning and smaller twinning feature dimensions are given by cursor plots C, J, and K respectively.

5.3 Prototypical Hydriding, Ion Milled

AFM imaging of a nickel plated Zircaloy-4 getter tube hydrided under prototypic conditions in D_2 at 350°C to a 0.5 H/Zr atomic ratio is shown in Figure 15. The sample was ion milled, according to the protocol outlined in section 3.2, resulting in a peak to valley height of ~150 nm, and RMS of 38.6 nm due to curtaining, Figure 15D. In addition to the large curtaining effects, individual SPPs shield regions downstream from the ion beam resulting in a ridge of residual Zr-4 material. While these effects are non-ideal for AFM imaging, at higher resolution (Figure 15G) they are less detrimental. As shown by SEM imaging, section 2.2, the hydride domains formed at this lower temperature are needle-like and penetrate through or deflect off of alpha Zr domains. Twinning, such as illustrated in Figure 14 above, was not observed by AFM imaging of needle-like hydride domains formed under these conditions. However, there was a fine structure in the needle-like hydrides, Figure 15H. Correlated SEM/AFM imaging is difficult, but possible as shown in Figure 15I-K. In future experiments fiducial markers should be employed to allow routine correlations between SEM and AFM.

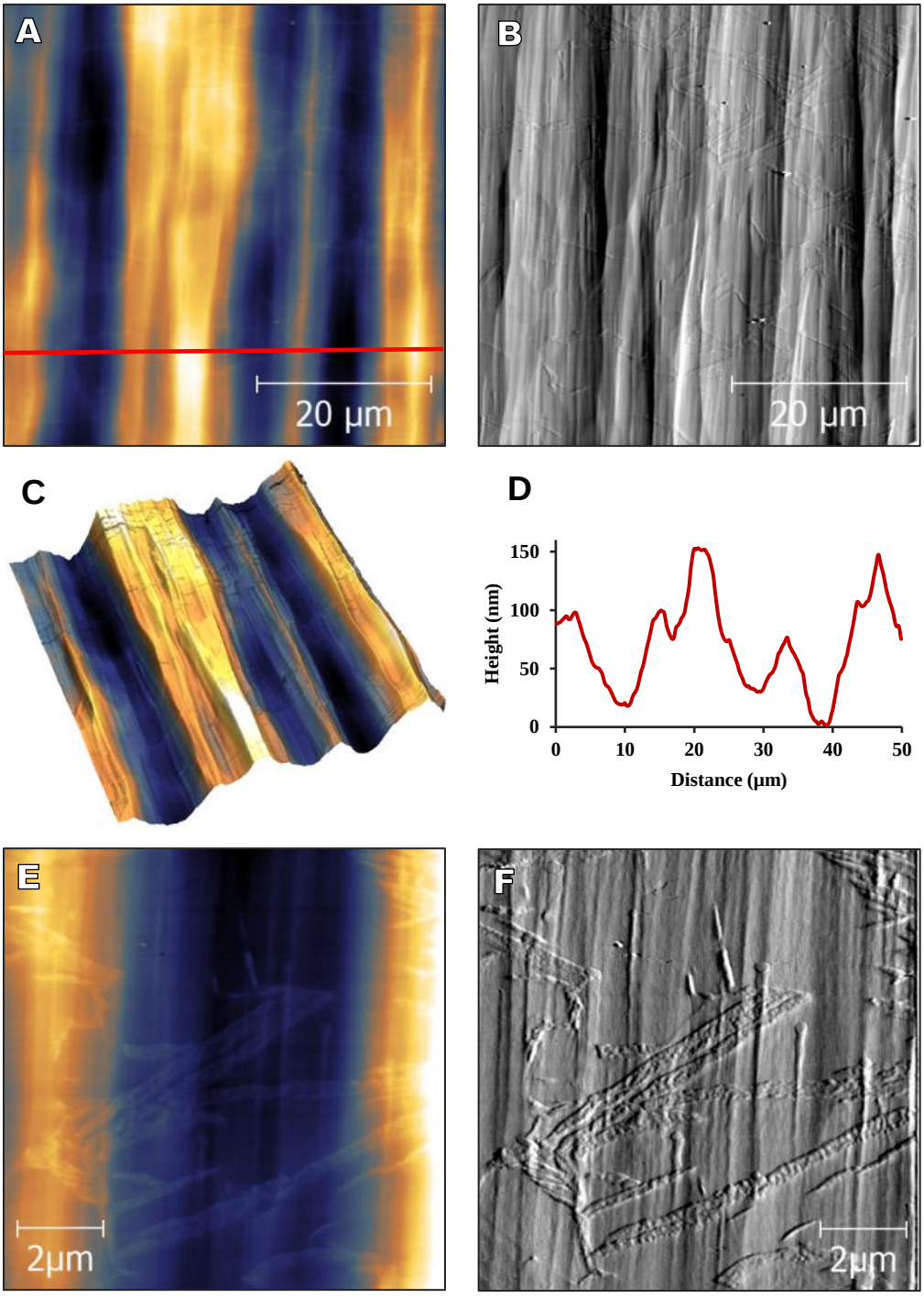
A
20 µm
B
20 µm
C
D
150
100
50
0
Height (nm)
0
10
20
30
40
50
Distance (µm)
E
2µm
F
2µm

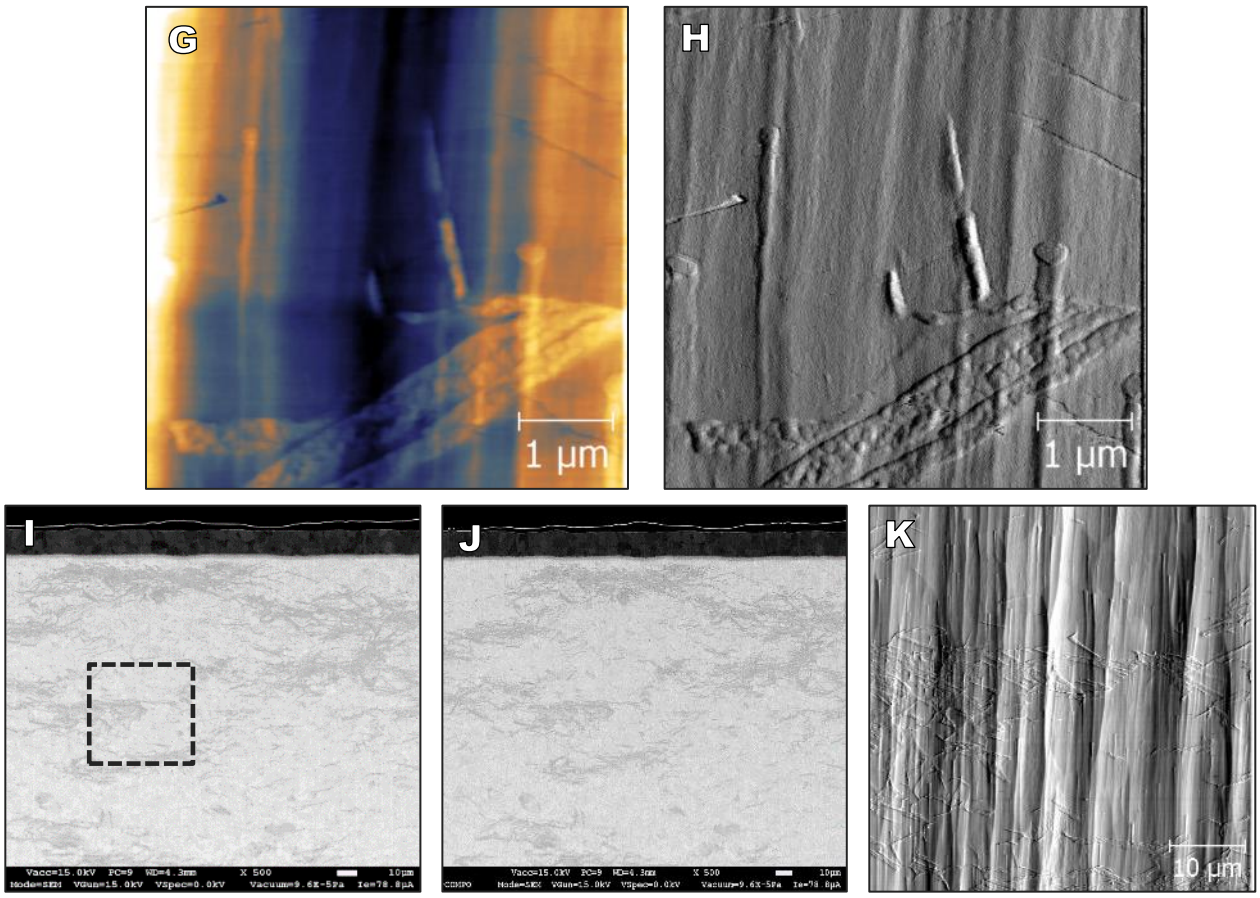

Figure 15. AFM topography (A, E, G), deflection (B, F, H), and 3D projection (C) images of hydride features present in an Ar-ion milled Zr-4 sample hydrided at 350°C. The large surface corrugation due to ion-mill curtaining are quantified in D. Correlative SEM/AFM imaging (I-K).

Mechanically polished Getter Rate samples were chosen for initial imaging with advanced AFM modes as they were typically flatter (no curtaining), the individual hydride domains were larger, and twinning was more prevalent.

5.4 Fast Force Mapping

Mechanical properties of surfaces, such as hardness, are traditionally measured by micro or nanoindentation. For example, Xu and Shi used these methods to interrogate the hardness of ZrH_x, Figure 17A-B.[5] While these methods provide valuable information they lack the ability to give domain specific values as microindentation interrogated a square region 55 µm across and nanoindentation a circle 870 nm in diameter, while most hydride domains are only a few hundred nanometers wide. Fast force mapping (FFM), however, utilizes an AFM tip to produce a high resolution map of force curves typically with 4 to 50 nm resolution. FFM utilizes the tip to probe the nano-mechanical features of a material in a manner similar to micro or nanoindentation. The tip is brought towards the surface until it presses onto the surface deflecting the cantilever up to a set value and is then retracted. By precisely measuring the spring constant of the cantilever beforehand, the deflection can be converted to an applied force plotted as a function of the vertical distance of the cantilever holder. The point of contact, curve slope and shape, displacement between approach and retract curves, and negative force values during retracting can be

used to determine the height, stiffness, deformation, and adhesion respectively at a single point on the surface, Figure 17A. Recent advances made with the MFP-3D Infinity allow a 512 by 512 grid of force curves to be captured in as little as 7 minutes in contrast to 36 hours required by previous instruments. In addition the high resolution nanomechanical data is mapped onto a topographical image generated at the same time such that non-representative regions such as domain boundaries and cracks can be identified and separated. The topography, relative hardness, and 3D relative hardness/topography overlay of individual domains of the Getter Rate sample measured using a silicon probe on a 26 N/m cantilever are shown in Figure 17A-C. The hardness of individual domains varies from 12.5 to 14.5 GPa. However, these values are not calibrated and should only be used to compare relative hardness between domains. Calculating quantitative values of hardness is difficult due to unknowns such as tip radius and shape. Future work should be done to carefully calibrate the hardness values given by each tip using known standards and comparisons with nanoindentation values on single crystal materials. In addition correlative SEM-EBSD should be used to accurately identify the hydride phase being interrogated, so that hardness values of individual hydride phases can be confidently determined. Previous studies using microindentation have reported hardness values of 1.6 GPa for α-Zr and 3 GPa for δ-ZrH while reported values using nanoindentation are 5.0 GPa for α-Zr and 3.5 GPa for ε-ZrH.[5,6] The increase in hardness of δ-ZrH relative to α-Zr is in agreement with the FFM results presented here. SEM-EBSD of the same sample reveals primarily δ-ZrH surrounding α-Zr which correlates well with the hardness map depicting thin regions of harder material surrounding softer material.

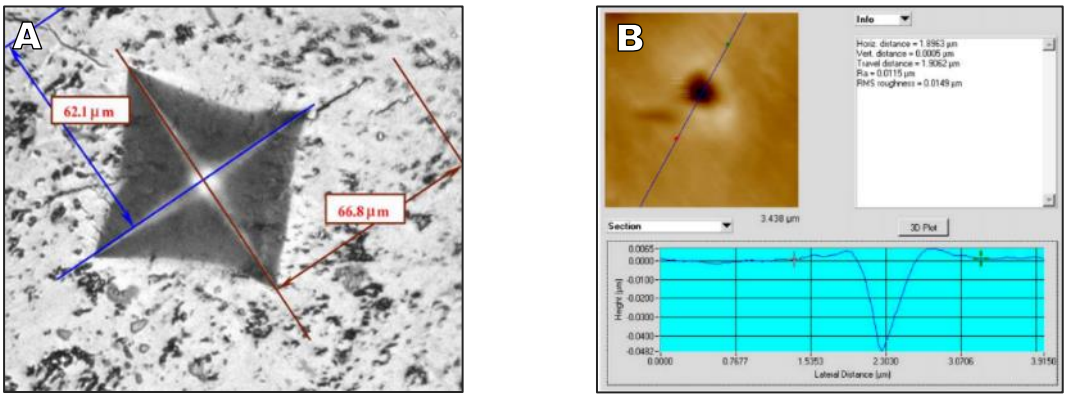

Figure 16. Microindentation (A) and nanoindentation (B) have been shown to provide mechanical properties of a region 55 µm square and 870 nm in diameter respectively.

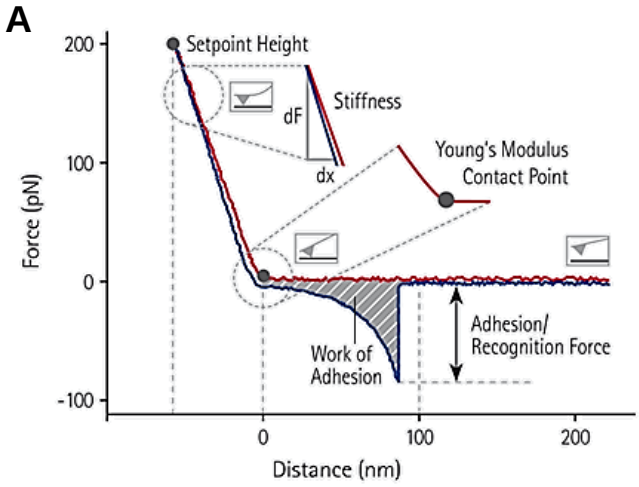

JPK Instruments QI Mode, https://usa.jpk.com

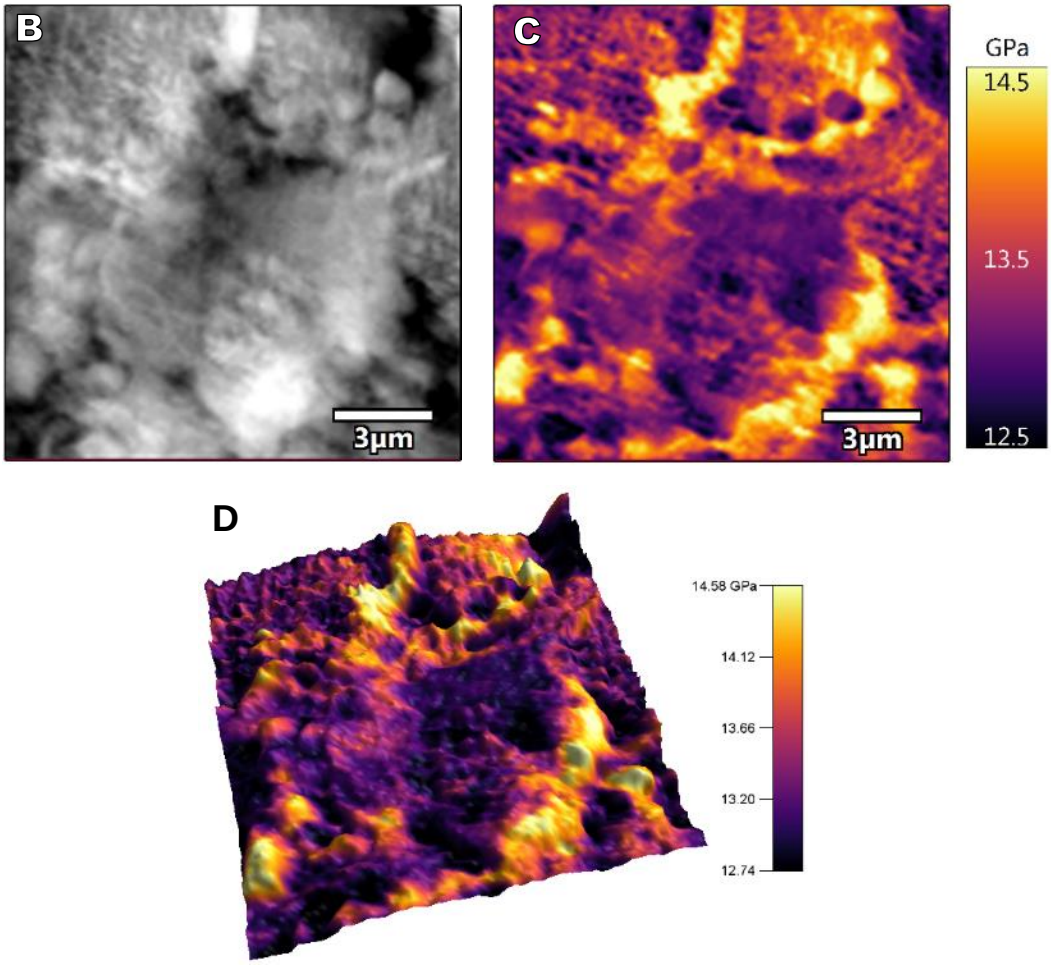

Figure 17. AFM based force curves provide mechanical properties at the nanometer scale (A). AFM topography (B), hardness (C), and hardness overlaid on a 3D projection of topography (D) of a mechanically polished Zr-4 sample hydrided at 500°C

5.5 Scanning Thermal Microscopy

By utilizing specialized thermocouple tips it is possible to measure the temperature of the tip during a scan. The cantilever and tip are heated by the deflected laser, such that decreases in the tip temperature while in contact with a sample are proportional to the thermal conductivity at the point of contact. The topography and resulting thermal maps of the Getter Rate sample are shown in Figure 18. The thermal signal contrast acquired is dependent on the set-point force applied while imaging as can be seen in the thermal maps acquired while imaging under a force of 50, 150, and 200 nN Figure 18B-D. The values given are relative values given by comparison to a single measured temperature. By careful calibration over a wide range of temperatures and comparisons to standards with known thermal properties, this technique can be developed to provide quantitative thermal conductivity of individual domains, and with correlative SEM-EBSD, with known hydride phases. It has been reported that the thermal conductivity of zirconium hydrides is lower than pure zirconium and decreases as the hydrogen content increases.[7] This is the opposite trend than was measured here. The lower temperature regions closely resemble the δ-ZrH regions revealed by SEM-EBSD of the same sample in a different region, Figure 18F. The cooler temperature of the (likely) hydride is indicative of a relatively *higher* thermal conductivity that causes the tip to lose heat at a greater rate relative to the surrounding α-Zr.

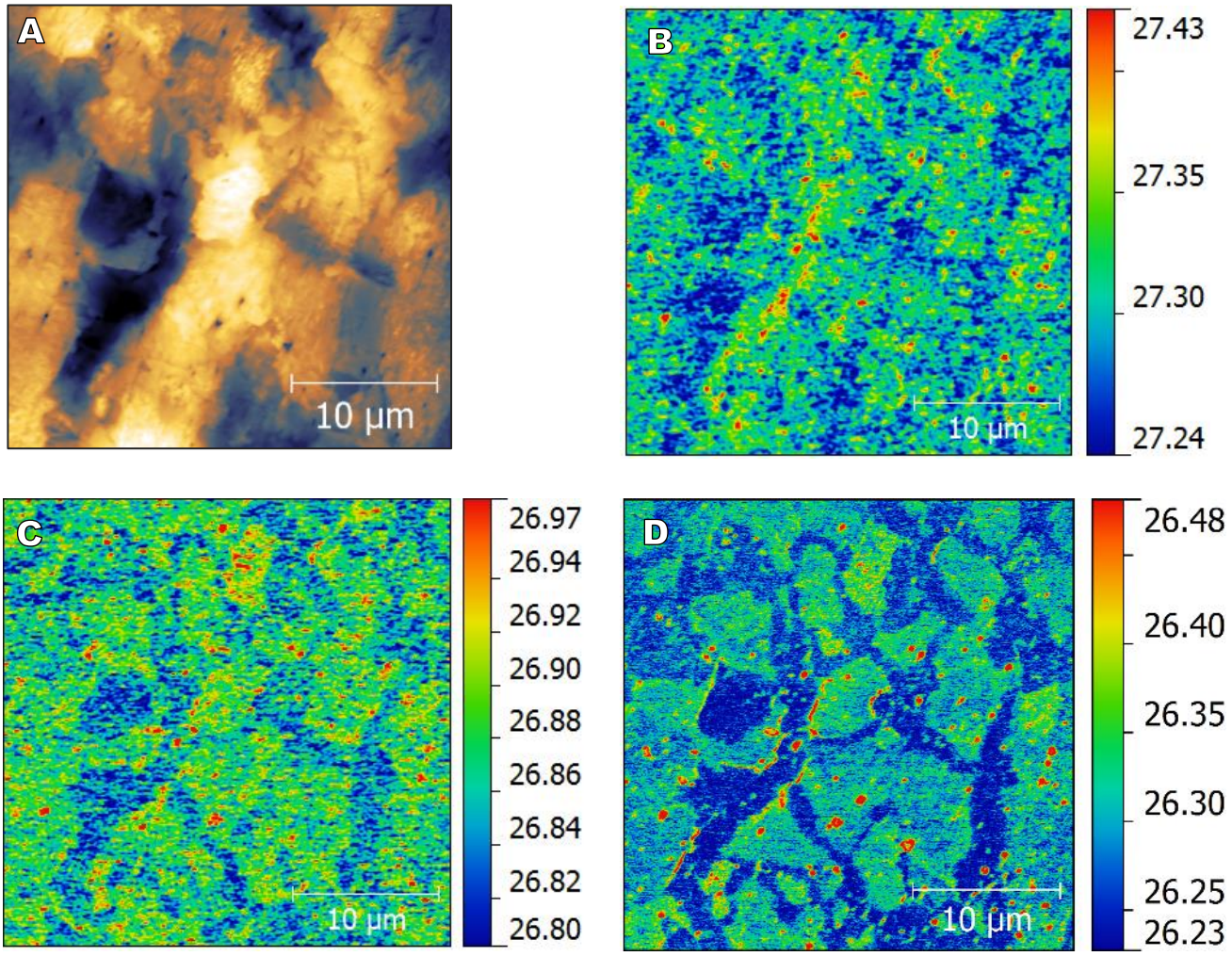

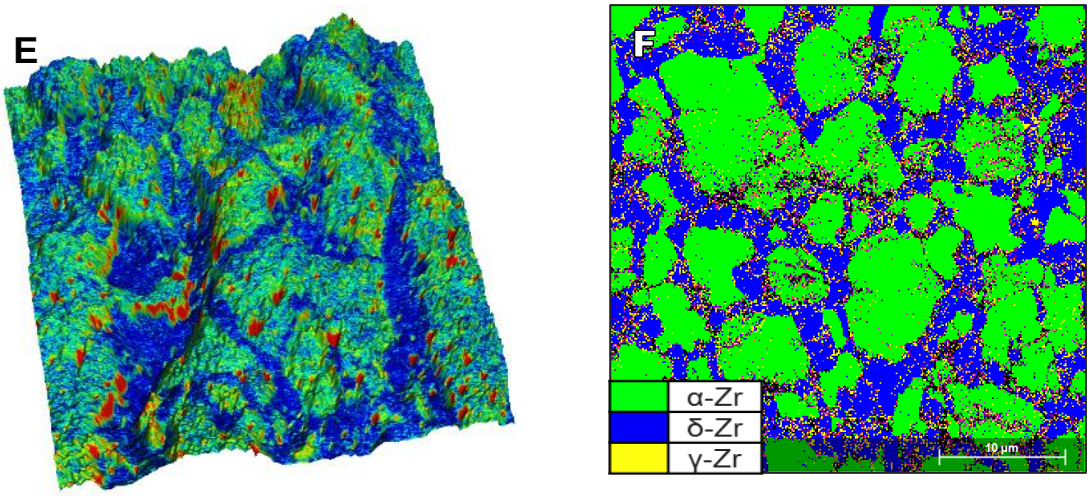

Figure 18. AFM topography (A), thermal maps acquired under 50 (B), 150 (C) and 200 nN (D), and thermal map D overlaid on a 3D projection of topography of a Zr-4 sample hydrided at 500°C and mechanically polished. The color scale temperature values are in degrees C. SEM-EBSD of a different region on the same sample reveals the phase of each domain (F).

5.6 Magnetic Force Microscopy

MFM is a two pass imaging technique where a magnetic tip is oscillated near the resonant frequency of the cantilever. On the first pass of each imaging line the topography is measured using the oscillation amplitude as the feedback mechanism. On the second pass the amplitude is decreased, the feedback is turned off, and the tip retraces the known topography of the surface at a set height while any change in frequency is passively monitored. Frequency shifts are a response by the oscillating magnetic tip to local magnetic domains in the sample. MFM analysis of the Getter Rate sample is shown in Figure 19. The amplitude channel (Figure 19A) depicts the topography of the surface collected on the first pass of the tip. As the tip scans from left to right, increases in local sample height briefly brings the tip closer to the surface decreasing the amplitude (dark regions) while decreases in local sample height cause an increase in amplitude (dark regions). In this way the edges of topographical features are highlighted. Changes in frequency during the second pass, caused by local magnetic domains, are shown in the magnetic channel, Figure 19B. The greatest magnetic response was located on and around the twinned hydride region with a positive shift corresponding to the twinned regions and a negative shift to the surrounding regions. This response may be due to opposite poles of magnetic domains present primarily in the twinned hydride region of the material. This result is surprising since it is reported that the magnetic susceptibility of hydrides is lower relative to pure zirconium and further decrease as a function of hydrogen content.[8] It is important to note that these domains are not merely a convolution of the topography as can be seen by overlaying the magnetic (frequency) channel onto the topography, Figure 19C. If care is not taken during MFM imaging to ensure the height of the probe is sufficient on the second (magnetic) pass, topographic features can cause a shift in frequency that will be convoluted with or overshadow the magnetic response. In this case if the contrast is adjusted correctly the first pass amplitude signal (topography) will resemble the magnetic channel as shown in Figure 19D-E.

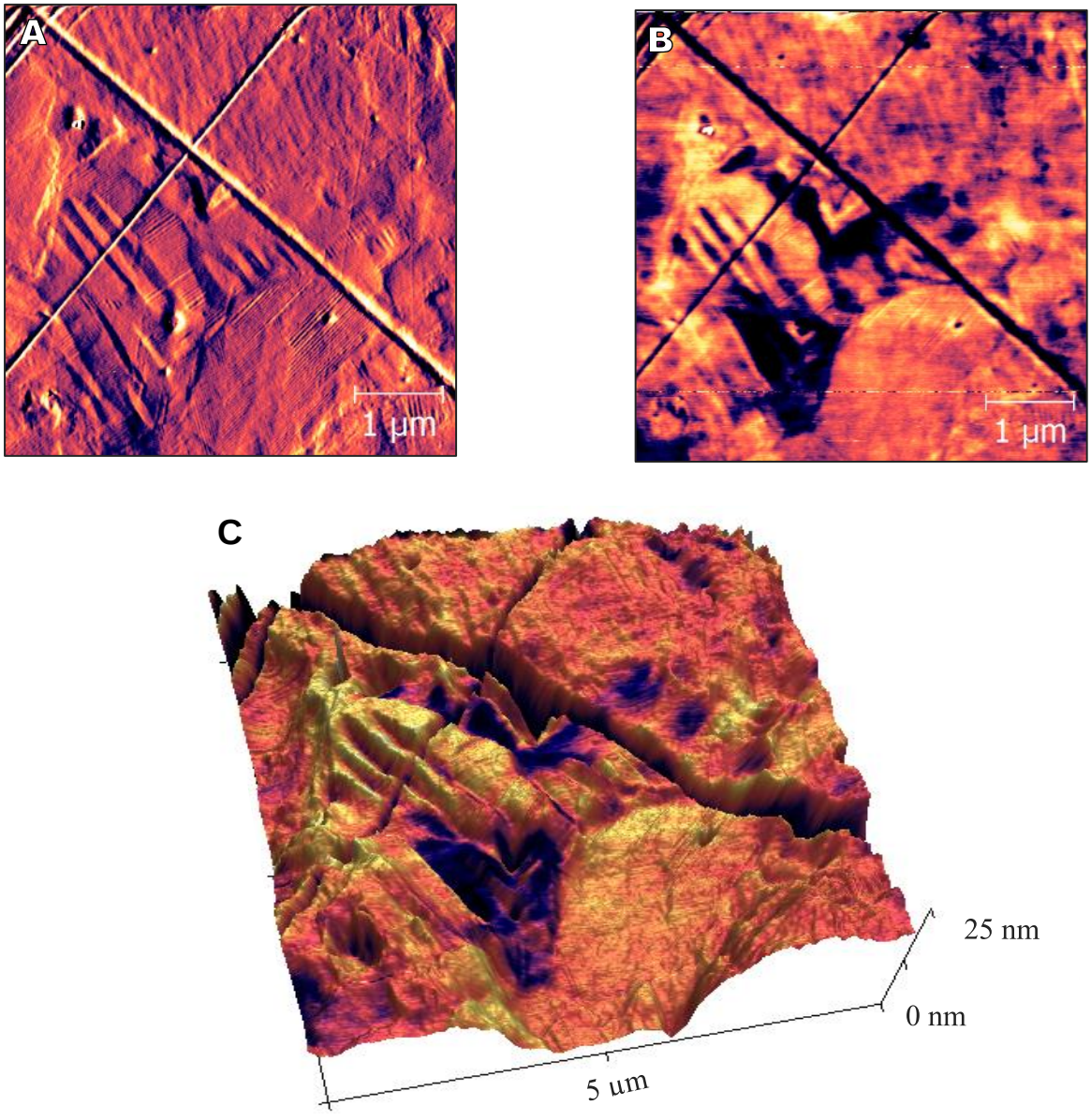
A
1 µm
B
1 µm
C
25 nm
0 nm
5 µm

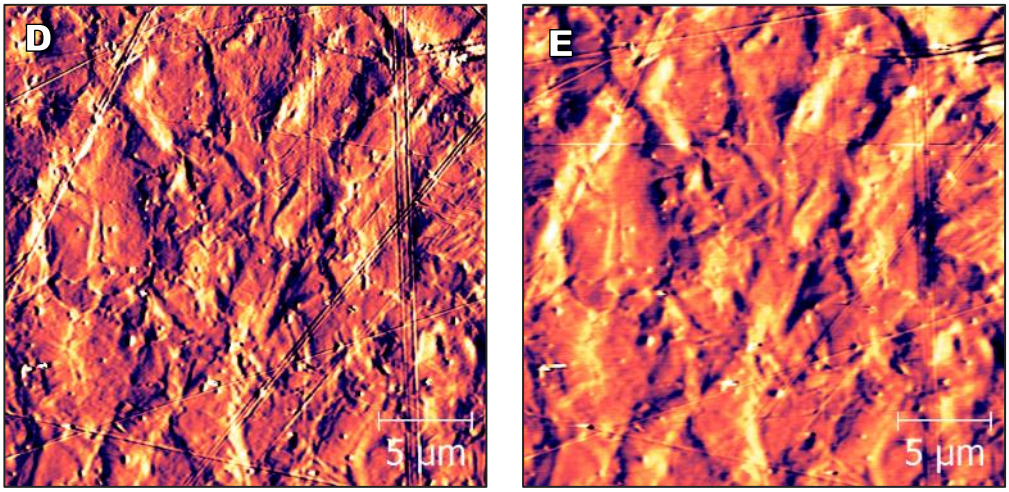

Figure 19. AFM amplitude (A), magnetic response (frequency) (B), and magnetic response overlaid onto a 3D projection of the topography (C) of a Zr-4 sample hydrided at 500°C and mechanically polished. If care is not taken during imaging the topography, as depicted by the amplitude channel (D), will be convoluted into the magnetic channel producing false magnetic domains (E), and cause the two channels to resemble one another.

6.0 Summary

Hydriding conditions play an important role in the hydride domains formed in Zircaloy 4. Previous work has shown that the primary factors involved are the hydrogen loading method and temperature. It was shown that while immersion loading produces a uniform distribution of hydrides, prototypic loading results in a gradient both axially and radially with a higher concentration in the central portion of the tube in the ID. Hydrides formed at 500°C typically form at α-Zr grain boundaries and can resemble α-Zr grains in size and structure. Hydrides formed at 350°C, however, grow parallel needle-like structures that penetrate α-Zr grains and tend to form in clusters. Both forms of hydride structures were found to exhibit twinning even at low hydrogen loading. In addition, two sample preparations have been developed with unique advantages and disadvantages. Mechanical polishing was found to produce relatively flat surfaces well suited to both SEM and AFM imaging. However, SEM analysis has shown that the Zr-4 surface can react with the polishing compounds. Ion-milling was shown to be free of these issues, producing clean surfaces that are well suited for EBSD mapping. However, significant curtaining complicates AFM imaging. It was found that additional surface cleaning was required for either method prior to AFM imaging.

AFM imaging provides quantification of the surface structure of the hydrided Zr-4 surfaces as prepared by mechanical polishing (7.5 nm RMS) and ion milling (38.6 nm RMS). Although ion-milling resulted in a rougher surface, high resolution AFM was still possible. Extensive twining was observed in hydrides formed at 500°C, but not in needle-like hydrides formed at 350°C. One of the several forms of twins that were observed consisted of hierarchical twins with larger ridges ~ 5 nm tall separated by 200-300 nm which were corrugated along one side with ~ 0.2 nm ridges separated by 20-30 nm. FFM of the Getter Rate sample successfully differentiated between surface domains, which appear to be α-Zr and hardened δ-ZrH. Likewise, SThM provided detailed thermal maps of individual domains showing that the δ-ZrH likely has a higher thermal conductivity. Finally, MFM revealed strong magnetic domains, which were mostly localized around regions of twinning. Correlated SEM/AFM of the same hydride domains was demonstrated paving the way for mapping material properties of known hydride phases. Overall, AFM has proved to be a useful tool for mapping domain specific material properties and microstructure and should be considered for further use in understanding fundamental properties of TPBAR components.

7.0 Future work

Correlative SEM/AFM analysis provides in depth insight into the fundamental properties of the chemical and physical nature of zirconium hydrides. Several improvements to the sample preparation and analysis should be pursued. These include:

- Take advantage of newly-acquired, state-of-the-art ion mill to produce flatter, surfaces free of chemical polishing artifacts and with reduced curtaining.
- Improved fiducial marking for ease of correlation between SEM and AFM analysis.
- Calibration of advanced AFM measurements (hardness, thermal conductivity, and possibly magnetic susceptibility) would allow for quantitative values that could be compared with other techniques and provide important parameters required for modeling.

Since the morphology of hydrides changes as a function of temperature, it would be useful to develop a correlation of hydride morphology and material properties as a function of temperature. This correlation could be valuable to understand and interpret PIE microstructures for getter tubes. Localized variations in hydride morphology could be used as an ex-situ indicator of localized temperature variations in the getter tube. This information would be valuable to know so it could be incorporated into more rigorous models of hydride formation. Suggested experiments include:

Conduct hydriding experiments at different temperatures using the two different hydriding set ups.

- Immersion hydriding at 350°C, 400°C, 450°C
- Prototypic hydriding at 400°C, 450°C, 500°C

Characterize the hydride microstructures using the following tools:

- SEM BSE to evaluate differences in hydride microstructure as a function of temperature.
- SEM BSE micrographs digitally processed based on contrast to compute area fraction of hydride phase vs. alpha phase. Does getter tube hydride to the same extent at different temperatures, or does the hydrogen migrate to other areas of the test set up?
- XRD and EBSD to characterize hydride phases formed. Do the same hydride phases form at different temperatures? Do they form in the same concentrations?
- AFM characterization of material properties. Do material properties of the same phase change as a function of domain size or hydriding conditions?

PIE analysis of irradiated getter tubes to determine the morphology and distribution of hydrides in order to determine the best hydrogen loading conditions to use for prototypic hydriding studies.

8.0 References

1. Johnson, B.R., McCarthy, B., Crum, J.V.; Examination of Hydrides Formed in the Zr-H System; TTP-3-710; Tritium Technology Program, 2015

2. Johnson, B.R., McCarthy, B., Crum, J.V., Elmore, M.R.; Zr-Hydride Phase Formation as a Function of Hydrogen Content; TTP-8-004; Tritium Technology Program, 2017

3. Johnson, B.R., McCarthy, J.V., Elmore, M.R.; Formation and Diffusion of Zirconium Hydrides in Nickle-plated Zircaloy-4 Tubing; PNNL-27232; Tritium Technology Program, 2018

4. Tewari, R., Srivastava, D., Dey, G.K., Chakravarty, J.K., Banergee, S., "Microstructural Evolution in Zirconium Based Alloys"; Journal of Nuclear Materials, 383, 153-171, 2008.

5. Xu, R., Shi, S.Q., "Investigation of mechanical properties of e-zirconium hydride using micro- and nano-indentation techniques", Journal of Nuclear Materials, 327, 165-170, 2004.

6. Yamanaka, S., Yoshioka, M., Uno, M., Katsura, H., Anada, T., Kobayashi, S., "Thermal and mechanical properties of zirconium hydride", Journal of Alloys and Compounds, 293, 23-29, 1999.

7. Uno, M., Yamada, K., Maruyama, T., Muta, H., Yamanaka, S., "Thermophysical properties of zirconium hydride and deuteride", Journal of Alloys and Compounds, 366, 101-106, 2004.

8. Bowman, R.C., Craft, B.D., Cantrell, J.S., Venturini, E.L., "Effects of thermal treatments on the lattice properties and electronic structure of ZrH_x", Physical Review B, 31, 5605-5615, 1985.

Pacific Northwest
NATIONAL LABORATORY

Proudly Operated by **Battelle** *Since 1965*

U.S. DEPARTMENT OF
ENERGY

902 Battelle Boulevard
P.O. Box 999
Richland, WA 99352
1-888-375-PNNL (7665)

www.pnnl.gov